
SoTeacher: A Student-oriented Teacher Network Training Framework for Knowledge Distillation

Chengyu Dong

University of California, San Diego
cdong@eng.ucsd.edu

Liyuan Liu

University of Illinois at Urbana-Champaign
ll2@illinois.edu

Jingbo Shang

University of California, San Diego
jshang@eng.ucsd.edu

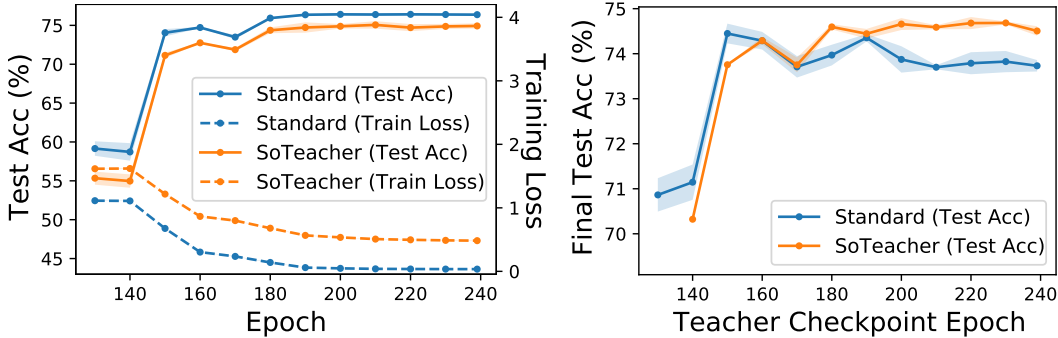
Abstract

How to train an ideal teacher for knowledge distillation is still an open problem. It has been widely observed that a teacher minimizing the empirical risk not necessarily yields the best performing student, suggesting a fundamental discrepancy between the common practice in teacher network training and the distillation objective. To fill this gap, we propose a novel student-oriented teacher network training framework SoTeacher, inspired by recent findings that student performance hinges on teacher’s capability to approximate the true label distribution of training samples. We theoretically established that (1) the empirical risk minimizer with proper scoring rules as loss function can provably approximate the true label distribution of training data if the hypothesis function is locally Lipschitz continuous around training samples; and (2) when data augmentation is employed for training, an additional constraint is required that the minimizer has to produce consistent predictions across augmented views of the same training input. In light of our theory, SoTeacher renovates the empirical risk minimization by incorporating Lipschitz regularization and consistency regularization. It is worth mentioning that SoTeacher is applicable to almost all teacher-student architecture pairs, requires no prior knowledge of the student upon teacher’s training, and induces almost no computation overhead. Experiments on two benchmark datasets confirm that SoTeacher can improve student performance significantly and consistently across various knowledge distillation algorithms and teacher-student pairs.

1 Introduction

In deep learning, knowledge distillation aims to train a small yet effective *student* neural network following the guidance of a large *teacher* neural network, typically based on the same training set Hinton et al. (2015). It dates back to the pioneer idea of model compression Buciluă et al. (2006) and has a wide spectrum of real-world applications, such as recommender systems Tang & Wang (2018); Zhang et al. (2020), molecular property prediction Hao et al. (2020), question answering systems Yang et al. (2020); Wang et al. (2020) and machine translation Liu et al. (2020).

Despite the prosper research interests in knowledge distillation, one of its crucial component, teacher training, remains largely unexplored. Existing training practice of teacher networks is often directly adopted from those aiming at their own performance, which not necessarily translates to student’s performance. Empirical evidences show that a teacher minimizing the empirical risk will yield an inferior student Cho & Hariharan (2019). As also shown in Figure 1, the teacher trained towards convergence will consistently reduce the performance of the student after a certain point. This



(a) Test accuracy and training loss of the teacher at different epochs through its training. (b) Student performance when distilled from different teacher checkpoints.

Figure 1: On CIFAR-100, we store a teacher checkpoint every 10 epochs and distill a student from it. We can observe that: (1) a standard teacher trained towards better teacher performance may consistently deteriorate student performance upon knowledge distillation; (2) a teacher trained using SoTeacher can achieve better student performance even with lower teacher performance.

suggests a fundamental discrepancy between the common practice in neural network training and the learning objective in knowledge distillation.

Recent advances have revealed that the student performance hinges on the quality of the soft predictions provided by the teacher, which ideally should approximate the true label distribution of the samples used in student training Menon et al. (2021); Dao et al. (2021). Thus, the first research question here is whether it is possible to learn the true label distribution of training data, especially when such distributions are usually unknown for real-world datasets. We give a positive answer by showing that the traditional empirical risk minimizer with proper scoring rules as loss functions can indeed approach the true label distribution of training data as long as the hypothesis function is locally Lipschitz continuous around training samples. The primary difference of such constraint to existing (robust) generalization theory is that we require the Lipschitz constraint be maintained at a larger scale, or more specifically across training inputs. We further show that when data augmentation is employed for training, additional constraint is required that the minimizer has to produce consistent predictions of the same training input after different augmentations.

In light of our theory, we propose a novel *student-oriented* teacher network training framework SoTeacher, which renovates the empirical risk minimization objective by incorporating Lipschitz regularization and consistency regularization. It is worth mentioning that SoTeacher is applicable to almost all teacher-student architecture pairs, requires no prior knowledge of the student upon teacher’s training, and induces almost no computation overhead.

We conduct extensive experiments on two benchmark datasets using various knowledge distillation algorithms and different teacher-student architecture pairs. The results confirm that SoTeacher can improve the student performance consistently and significantly.

To summarize, our main contributions can be listed as follows.

- We show the theoretical feasibility of learning the true label distribution of training data in teacher training, in order to improve the student performance. To the best of our knowledge, such learning problem focusing on training data lacks discussion in the literature since most traditional tasks target the performance on the unseen test data.
- We propose a novel student-oriented teacher training framework SoTeacher by incorporating Lipschitz regularization and consistency regularization into teacher training. It can be applied to almost all teacher-student architecture pairs with almost no computation overhead.
- Extensive experiments on two benchmark datasets have confirmed the superiority of SoTeacher.

2 Related work

Understand knowledge distillation. Knowledge distillation is a widely applicable technique for model compression. However, its underlying mechanism is still not clear, especially given the empirical observations that improving teacher performance not necessarily improves student

performance Müller et al. (2019); Cho & Hariharan (2019). Derived from the intuition about the “dark knowledge” Hinton et al. (2015), recent works have shown that the effectiveness of knowledge distillation from a statistical perspective. In specific, Menon et al. (2021) show that the predictive distribution of the teacher is essentially an approximation to the true label distribution, and true label distribution as a supervision for the student improve the generalization bound compared to one-hot labels. Dao et al. (2021) show that the accuracy of the student is directly bounded by the distance between teacher’s prediction and the true label distribution through the Rademacher analysis. These analyses thus establish the formal criterion of an ideal teacher, namely approximation error of its predictions to the true label distribution on student’s training data. This also implies that a teacher trained towards convergence may not be beneficial to the student.

Intuitively, it is possible to tackle this problem by early stop Cho & Hariharan (2019). However, meticulous hyperparameter search may be required since the best checkpoint is often sensitive to the epoch and varies across different training settings such as the learning rate scheduler. It is also possible to save multiple early checkpoints for the student to be distilled from sequentially Jin et al. (2019), which is orthogonal to and can thus also benefit from our teacher training strategy. With an complete overhaul of current teacher training practice while at the cost of increased computation, one can utilize a “cross-fitting” procedure to prevent teacher memorizing the training data. Namely the training data is first partitioned into several folds, where the teacher predictions on each fold is generated based on the teacher trained only on out-of-fold data Dao et al. (2021). In case of the student architecture is known at the teacher training time, one can augment the teacher network with student’s network blocks and train them jointly. The teacher can thus be trained with reference to the student performance, instead of solely towards its own performance Park et al. (2021). For multi-generation knowledge distillation specifically Furlanello et al. (2018), one can penalize the difference between the predictive probability at the true class and the probabilities at other semantically relevant classes to encourage the learning of secondary probabilities in teacher’s prediction, which is shown to improve the performance of models in later generations Yang et al. (2019)

Different from these attempts, we propose a practically feasible student-oriented teacher training framework, with minimum computation overhead and no prior knowledge of the student architecture.

Uncertainty estimation on unseen data. Since the objective of our student-oriented teacher training is to learn label distributions of the training data, it might be related to those methods aiming to learn quality uncertainty on the unseen data. We consider those methods that are practically feasible for large teacher network training, including (1) classic statistical approaches to overcome overfitting such as ℓ_1 and ℓ_2 regularization, (2) modern regularization methods such as label smoothing Szegedy et al. (2016) and data augmentation approaches such as mixup Zhang et al. (2018a) and Augmix Hendrycks et al. (2020), (3) Post-training methods such as temperature scaling Guo et al. (2017), as well as (4) methods that incorporate uncertainty as a learning objective such as confidence-aware learning (CRL) Moon et al. (2020).

We have conducted experiments on CIFAR-100 using all these methods and the results can be found in Appendix D. Unfortunately, the performance of these regularization methods is unsatisfactory in knowledge distillation — only CRL can slightly outperform the standard training. We believe the reasons might be two-folds. First, most existing criteria for uncertainty quality on the unseen data such as calibration error Naeini et al. (2015) or ranking error Geifman et al. (2019), only require the model to output an uncertainty estimate that is correlated with the probability of incorrect predictions. Such criteria may not be translated into the approximation error to the true label distribution. Second, even if a model learns true label distribution on unseen data, it not necessarily has to learn true label distribution on the training data, as deep neural networks tends to memorize the training data.

3 Problem Formulation

Multi-class classification. Here, we study knowledge distillation in the context of multi-class classification. Specifically, we are given a set of training samples $\mathcal{D} = \{(x_i, y_i)\}_{i=1}^N$ drawn from a probability distribution $p_{X,Y}$ defined jointly over input space $\mathcal{X} \subset \mathbb{R}^d$ and label space $\mathcal{Y} = \{1, 2, \dots, K\}$. The goal is to learn a function f that maps the inputs to the labels.

Common practice in neural network training. Given the set of training examples \mathcal{D} , one typically solves the function \mathbf{f} by minimizing the *empirical risk*, namely

$$\mathbf{f}^* = \arg \min_{\mathbf{f}} \frac{1}{N} \sum_i \ell(\mathbf{f}(x_i), y_i). \quad (1)$$

Our Research Questions. In this paper, we present our findings of the following two questions in Sec. 4 and Sec. 5, respectively.

- (i) *Can a teacher network learn the true label distribution of the training data under the empirical risk minimization framework?*
- (ii) *How to train a teacher towards the student performance without significant deviation from the existing teacher training practice?*

4 Theoretical Feasibility to Learn True Label Distribution of Training Data

We now explore the theoretical feasibility of training a teacher that predicts the true label distribution of the training data. We do not intend a complete overhaul of the training practice of large neural networks. Therefore we restrict our exploration to the possible constraints imposed on the empirical risk minimization that leads to minimizers approximating the true label distribution. Note that throughout the discussion here, our major focus is the *existence* of such proper minimizers, instead of how to achieve them, which concerns more about the details of the optimization process.

We begin our analyses by observing that the label y of an training input x distributes according to its true label distribution, namely $y|x \sim p_{Y|X}(y|x)$ and $\mathbb{E}[\mathbf{1}_y] = \mathbf{p}^*(x) \equiv p_{Y|X}(\cdot|x)$ Neal (2007). Thus given a collection of training inputs with the same true label distribution $\mathcal{S}(\mathbf{q}) = \{(x, y) \mid \mathbf{p}^*(x) = \mathbf{q}\}$, the sample mean of their one-hot labels $\bar{\mathbf{y}} = |\mathcal{S}(\mathbf{q})|^{-1} \sum_x \mathbf{1}_y$ converges to the true label distribution.

Now given an ideal condition that the predictions of training inputs in $\mathcal{S}(\mathbf{q})$ are always identical, the empirical risk will attain the minimum when the predictions are equal to the sample mean, as long as the loss function is a proper scoring rule Gneiting & Raftery (2007); Lakshminarayanan et al. (2017). In specific, if for all $x \in \mathcal{S}(\mathbf{q})$, $\mathbf{f}(x) = \mathbf{p}$, then

$$\frac{1}{|\mathcal{S}(\mathbf{q})|} \sum_x \ell(\mathbf{f}(x), y) = \ell(\mathbf{p}, \bar{\mathbf{y}}) + \ell_c(\bar{\mathbf{y}}) \geq \ell(\bar{\mathbf{y}}, \bar{\mathbf{y}}) + \ell_c(\bar{\mathbf{y}}), \quad (2)$$

with equality if and only if $\mathbf{p} = \bar{\mathbf{y}}$, where ℓ_c is a constant that only depends on $\bar{\mathbf{y}}$. For example, if ℓ is the negative-log likelihood loss (NLL), by Gibbs' inequality we have

$$\frac{1}{|\mathcal{S}(\mathbf{q})|} \sum_x -\mathbf{1}_y \cdot \log \mathbf{f}(x) = -\bar{\mathbf{y}} \cdot \log \mathbf{p} \geq -\bar{\mathbf{y}} \cdot \log \bar{\mathbf{y}}. \quad (3)$$

Or if ℓ is Mean Squared Error (MSE) (or known as the Brier score Brier (1950)), we have

$$\frac{1}{|\mathcal{S}(\mathbf{q})|} \sum_x \|\mathbf{1}_y - \mathbf{f}(x)\|_2^2 = \|\bar{\mathbf{y}} - \mathbf{p}\|_2^2 + (1 - \|\bar{\mathbf{y}}\|_2^2) \geq 1 - \|\bar{\mathbf{y}}\|_2^2. \quad (4)$$

However, in a realistic scenario the true label distribution is unknown, therefore it is not possible to (i) identify training inputs with the same true label distribution, (ii) enforce their predictions to be identical. To this end, we investigate the empirical risk minimization locally in a subset of the training inputs where all inputs are close to each other. Mathematically these subsets can be created by using a metric ball of radius r to cover the entire training set. We then show that ideal conditions (i) and (ii) can be relaxed to be more realistic settings.

- (i) We show that in such subsets as long as the training inputs have similar true label distributions, their individual true label distributions will be close to their sample mean. This can be established by assuming the true label distribution is locally-Lipschitz continuous.
- (ii) We show that in such subsets as long as training inputs have similar predictions, the minimum of the empirical risk is attained only if the predictions are close to the sample mean. This amounts to restricting the hypothesis functions to be locally-Lipschitz continuous around training inputs.

Combine (i) and (ii) we can then show that the minimizer of the empirical risk will produce predictions on training inputs close to their true label distributions.

Now we are ready to present our main theorem. The above relaxations will be discussed in detail through its proof in Appendix A.

Theorem 4.1 (Approximation error of the empirical risk minimizer to the true label distribution). *Assume the function generating the true label distribution $\mathbf{p}^* : \mathcal{X} \rightarrow \mathcal{Y}$ is L^* -locally Lipschitz continuous in a norm ball of radius r around $x \in \mathcal{X}$. Select the loss function $\ell(\cdot, \cdot)$ to be a proper scoring rule. Denote $\mathcal{S} = \{x_i\}_{i \leq N}$ as the collection of all training inputs. Let $\mathcal{C}^r = \{\bar{x}_j\}_{j \leq N_r}$ be an r -external covering of \mathcal{S} . Let $\{\mathcal{S}_j^r\}_{j \leq N_r}$ be a disjoint partition of \mathcal{S} induced by \mathcal{C}^r . Let $\mathcal{F}_{L,r}$ be a family of functions that are L -locally Lipschitz continuous in a norm ball of radius r around $x \in \mathcal{C}^r$. Let $\mathbf{f}^* \in \mathcal{F}_{L,r}$ be a function that minimizes the empirical risk, namely $\mathbf{f}^* = \arg \min_{\mathbf{f} \in \mathcal{F}_{L,r}} \hat{R}(\mathbf{f}, \mathcal{S})$, where the empirical risk is,*

$$\hat{R}(\mathbf{f}, \mathcal{S}) = \frac{1}{N} \sum_{i=1}^N \ell(\mathbf{f}(x_i), y_i). \quad (5)$$

Let $\kappa \geq 1$ be a number and $\tilde{\mathcal{S}}$ be a subset of \mathcal{S} with cardinality at least $(1 - 1/\kappa + 1/(\kappa N^r))N$. Then for any $x \in \tilde{\mathcal{S}}$, any p -norm $\|\cdot\|$, and any $\varepsilon > 0$, with probability at least $1 - \delta$, we have

$$\|\mathbf{f}^*(x) - \mathbf{p}^*(x)\| \leq \sqrt{\frac{2\kappa N^r K}{N} \log \frac{2}{\delta}} + Lr(1 + K\|\mathbf{1}_{(\cdot)} - K^{-1}\mathbf{1}\|) + 2L^*r \quad (6)$$

Here $\mathbf{1}_{(\cdot)} \in \mathbb{R}^K$ denotes the vector where an arbitrary entry is 1 and others are 0, and $\mathbf{1} \in \mathbb{R}^K$ denotes the vector where all entries are 1. And K is the number of classes.

One can find that as long as L^* and L are small enough, and the size of the training set N is sufficiently large, for a majority of the training inputs the predictions can approach the true label distribution with high probability. Interestingly, (6) also shows that the bound will be tighter if the number of classes K is small, which implies learning the true label distribution of the training data will be significantly easier on classification tasks with few classes.

4.1 The case with data augmentation

When data augmentation is employed in training we note that the difference between the predictions of empirical risk minimizer and the true label distribution of the training inputs can be bounded similarly. Following the proof of Theorem 4.1, we first partition the augmented training set in a way such that all augmented views of an input x are grouped into the previous subset \mathcal{S}_j^r containing x . Therefore we can ensure the covering number will not increase. Then we can observe that the differences to the proof of Theorem 4.1 come from two parts. First, we require the true label distributions of all augmented inputs to be close to that of the original input. Second, we require the predictions of all augmented inputs to be close to that of the original input. These two induces additional two error terms. We have the following theorem.

Theorem 4.2 (Error of empirical loss minimization with data augmentation). *Consider the same setting as Theorem 4.1, except each training input is now augmented by a set of operator $\{A_m\}_{m \leq M}$. Now the collection of all training inputs becomes $\mathcal{S}_A = \bigcup_{i \leq N} \{A_m(x_i)\}_{m \leq M}$, and the empirical risk becomes*

$$\hat{R}(\mathbf{f}, \mathcal{S}_A) = \frac{1}{NM} \sum_{i=1}^N \sum_{m=1}^M \ell(\mathbf{f}(A_m(x_i)), y_i) \quad (7)$$

Then the empirical risk minimizer $\mathbf{f}^* = \arg \min_{\mathbf{f} \in \mathcal{F}_{L,r}} \hat{R}(\mathbf{f}, \mathcal{S}_A)$ has the property that, with probability at least $1 - \delta$,

$$\|\mathbf{f}^*(x) - \mathbf{p}^*(x)\| \leq \sqrt{\frac{2\kappa N^r K}{N} \log \frac{2}{\delta}} + Lr\xi_K + 2L^*r + L_f^A \xi_K + L_p^A, \quad (8)$$

where $\xi_K = (1 + K\|\mathbf{1}_{(\cdot)} - K^{-1}\mathbf{1}\|)$, $L_f^A = \max_{i,m} \|\mathbf{f}^*(A_m(x_i)) - \mathbf{f}^*(x)\|$, $L_p^A = \max_{i,m} \|\mathbf{p}^*(A_m(x_i)) - \mathbf{p}^*(x)\|$.

Theorem 4.2 suggests that to ensure the learning of true label distribution with data augmentation, one has to explicitly minimize two additional error terms. Here L_f^A and L_p^A cannot be simply bounded by the local Lipschitz continuities of the hypothesis function and true label distribution respectively, because the augmentation operator can significantly change the data matrix of the input, which means $\|A(x) - x\|$ is not necessarily small.

Note that although the training set is larger after augmentation, the bound (8) is not improved by a multiplier compared to the case with no augmentation (6). This is because the one-hot labels of augmented inputs are statistically dependent, thus the concentration inequality (Lemma A.2) will not become tighter.

5 Student-oriented Teacher Network Training Framework

Following our theory in Sec. 4, we propose a novel *student-oriented* teacher network training framework SoTeacher. It renovates the traditional empirical risk minimization by incorporating Lipschitz regularization and consistency regularization, such that the teacher is trained to approximate the true label distribution of training data, thus benefiting the generalization of the student.

Lipschitz regularization. First, by Theorem 4.1 the necessary conditions to ensure the empirical risk minimization can approach the true label distribution are (i) selecting a proper scoring rule as the loss function (ii) enforcing the hypothesis function to be locally Lipschitz continuous around certain samples. The former can be sufficed by selecting loss functions such as the cross-entropy loss and MSE used in existing training practice. The latter can be achieved by simply impose a global Lipschitz constraint, which amounts to introducing Lipschitz regularization (LR) into teacher’s training. Here it is important to enforce more stringent Lipschitz constraint than that required by generalization to unseen data.

Following previous practice using Lipschitz regularization for generalization on unseen data Yoshida & Miyato (2017) or stabilizing generative model Miyato et al. (2018), we regularize the Lipschitz constant of a network by constraining the Lipschitz constant of each trainable component. The regularization term is thus defined as

$$\ell_{\text{LR}} = \sum_f \text{Lip}(f), \quad (9)$$

where f denotes a trainable component in the network \mathbf{f} . The Lipschitz constant of a network component $\text{Lip}(f)$ induced by a norm $\|\cdot\|$ is the smallest value L such that for any input features h, h' ,

$$\|f(h) - f(h')\| \leq L\|h - h'\|. \quad (10)$$

Here we adopt the Lipschitz constant induced by 1-norm, since its calculation is accurate, simple and efficient. For calculating the Lipschitz constants of common trainable components in deep neural networks, we refer to Gouk et al. (2021) for a comprehensive study.

Consistency regularization. Second, based on Theorem 4.2, when data augmentation is employed in training it is necessary to (i) ensure the true label distribution of an input will not change significantly after data augmentations (ii) ensure teacher’s predictions of an input will not change significantly after data augmentations. The former can be sufficed by selecting data augmentations such as random cropping, rotation or flipping commonly seen in the training practice. The latter is known as the consistency regularization (CR) Laine & Aila (2017); Xie et al. (2020); Berthelot et al. (2019); Sohn et al. (2020) that is widely used in semi-supervised learning. To maximize the training efficiency for large teacher network, we utilize temporal ensembling Laine & Aila (2017), namely penalizing the difference between the current prediction and the aggregation of previous predictions for each training input. In this way the consistency under data augmentation is implicitly regularized since the augmentation is randomly sampled in each epoch. And it is also efficient as no extra model evaluation is required for an input.

Therefore, we design our consistency regularization term as

$$\ell_{\text{CR}} = \frac{1}{N} \sum_i \left\| \mathbf{f}(x_i) - \overline{\mathbf{f}(x_i)} \right\|_2^2. \quad (11)$$

where we follow previous work Laine & Aila (2017) and employ MSE to penalize the difference. Here $\overline{\mathbf{f}(x)}$ is the aggregated prediction of an input x , which we calculate as the simple average of previous predictions

$$\overline{\mathbf{f}(x)}_t = \frac{1}{t} \sum_{t'=0}^{t-1} \mathbf{f}(x)_{t'}, \quad (12)$$

where we omit the data augmentation operator for simplicity. At epoch 0 we simply skip the consistency regularization. Note that (12) can be implemented as an online average thus there is no need to store every previous prediction of an input.

To scale the consistency loss terms, a weight is often adjusted based on a Gaussian ramp-up curve in previous works Laine & Aila (2017). However, the specific parameterization of such a Gaussian curve varies greatly across different implementations, where more than one additional hyperparameters are set up and tuned heuristically. Here to avoid tedious hyperparameter tuning we simply linearly interpolate the weight from 0 to its maximum value, namely

$$\lambda_{\text{CR}}(t) = \frac{t}{T} \lambda_{\text{CR}}^{\text{max}}, \quad (13)$$

where T is the total number of epochs.

Summary. To recap, our teacher training strategy introduces two additional regularization terms. The loss function can thus be defined as

$$\ell = \ell_{\text{Stand.}} + \lambda_{\text{LR}} \ell_{\text{LR}} + \lambda_{\text{CR}} \ell_{\text{CR}}, \quad (14)$$

where $\ell_{\text{Stand.}}$ is the standard empirical risk defined in (1). Our strategy is simple to implement and requires no prior knowledge of the specific student architectures in the subsequent distillation process. It also incurs only minimal computation overhead (see Section 6.2). Therefore we believe our strategy can be readily built into the training practice of large neural networks.

6 Experiments

In this section we evaluate the effectiveness of SoTeacher on teacher training in knowledge distillation. We focus on model compression from a large network to a smaller one, where the student is trained on the same data set as the teacher, thus is well-supported by our theoretical understanding.

6.1 Experiment setup

Datasets. In our experiments, we use two benchmark datasets: (1) CIFAR-100 Krizhevsky (2009) consists of 50,000 training samples from 100 classes; and (2) Tiny-ImageNet Tin (2017) is a miniature version of ImageNet Deng et al. (2009) consisting of 100,000 training samples selected from 200 classes. Due to computational constraints, we were not able to conduct experiments on ImageNet. Most of our experimental results are from CIFAR-100, and Tiny-ImageNet mainly serves as the second dataset to validate our claims.

Compared Methods. We denote our novel student-oriented teacher network training framework as **SoTeacher**. We compare SoTeacher with the common teacher training practice (*i.e.*, Eq. 1) in knowledge distillation (denoted as **Standard**).

For ablation study, we toggle off the Lipschitz regularization (LR) or consistency regularization (CR) in SoTeacher (denoted as **no-LR** and **no-CR**, respectively) to explore their individual effects and the necessity of including both of them.

Teacher-Student Pairs. On CIFAR-100, we experiment with various network backbones including ResNet He et al. (2016), Wide ResNet Zagoruyko & Komodakis (2016) and ShuffleNet Zhang et al. (2018b); Tan et al. (2019). To test the applicability our method, we consider different aspects of model compression in knowledge distillation including reduction of the width or depth, and distillation between heterogeneous neural architectures. Due to space constraints, we select representative teacher-student pairs including WRN40-2/WRN40-1, WRN40-2/WRN16-2, and ResNet32x4/ShuffleNetV2 to reflect all these aspects. On Tiny-ImageNet, we conduct knowledge distillation between ResNet34 and ResNet18.

Table 1: Results on CIFAR-100 using KD as the knowledge distillation algorithm and various architectures. SoTeacher achieves better student accuracy than Standard with a lower teacher accuracy.

	WRN40-2/WRN40-1		WRN40-2/WRN16-2		ResNet32x4/ShuffleNetV2	
	Student	Teacher	Student	Teacher	Student	Teacher
Standard	73.73 \pm 0.13	76.38 \pm 0.13	74.87 \pm 0.45	76.38 \pm 0.13	74.86 \pm 0.18	79.22 \pm 0.03
SoTeacher	74.35 \pm 0.23	74.95 \pm 0.28	75.39 \pm 0.23	74.95 \pm 0.28	77.24 \pm 0.09	78.49 \pm 0.09
no-CR	74.34 \pm 0.11	74.30 \pm 0.12	75.20 \pm 0.24	74.30 \pm 0.12	76.52 \pm 0.52	77.73 \pm 0.17
no-LR	73.81 \pm 0.15	76.71 \pm 0.16	75.21 \pm 0.13	76.71 \pm 0.16	76.23 \pm 0.18	80.01 \pm 0.18

Table 2: Results on Tiny-ImageNet using KD as the knowledge distillation algorithm. The teacher network is ResNet34 and the student network is ResNet18. SoTeacher achieves better student accuracy than Standard with a lower teacher Top-1 accuracy.

	Student (Top-1)	Student (Top-5)	Teacher (Top-1)	Teacher (Top-5)
Standard	66.19 \pm 0.17	85.74 \pm 0.21	64.94 \pm 0.32	84.33 \pm 0.40
SoTeacher	66.83 \pm 0.20	86.19 \pm 0.22	64.88 \pm 0.48	84.91 \pm 0.41
no-CR	66.39 \pm 0.27	86.05 \pm 0.17	64.36 \pm 0.43	84.10 \pm 0.27
no-LR	66.48 \pm 0.43	86.20 \pm 0.40	64.26 \pm 1.54	84.48 \pm 0.84

Knowledge Distillation Algorithms. We experiment with the original knowledge distillation method (KD) Hinton et al. (2015), and a wide variety of other sophisticated knowledge distillation algorithms including FitNets Romero et al. (2015), AT Zagoruyko & Komodakis (2017), SP Tung & Mori (2019), CC Peng et al. (2019), VID Ahn et al. (2019), RKD Park et al. (2019), PKT Passalis & Tefas (2018), AB Heo et al. (2019), FT Kim et al. (2018), NST Huang & Wang (2017), CRD Tian et al. (2020), SSKD Xu et al. (2020) and RCO Jin et al. (2019). For the implementation of these algorithms, we refer to existing repositories for knowledge distillation Tian et al. (2020); Shah et al. (2020); Matsubara (2021) and author-provided codes.

Evaluation Metrics. We report the teacher performance and the resulted student performance of the last teacher checkpoint. The performance is always evaluated on the test set from 3 runs using different random seeds. We present both mean and standard deviation of the test accuracy. For Tiny-ImageNet we also report the top-5 accuracy following the common setting.

Hyperparameter Settings. For our teacher training method, we set $\lambda_{CR}^{max} = 1$ for both datasets. For Lipschitz regularization, we set $\lambda_{LR} = 10^{-5}$ for CIFAR-100 and $\lambda_{LR} = 10^{-6}$ for Tiny-ImageNet, as the regularization term is the sum of the Lipschitz constants of trainable parameters, and the teacher model for Tiny-ImageNet has approximately 10 times more parameters than that for CIFAR-100. More detailed hyperparameter settings for neural network training and knowledge distillation algorithms can be found in Appendix C.

6.2 Results

With KD as the knowledge distillation algorithms, Table 1 and 2 show the evaluation results on CIFAR-100 and Tiny-ImageNet, respectively. This table cover four different teacher/student architecture pairs and provide detailed numbers for both teacher and student test results. Table 3 shows the evaluation results on CIFAR-100 with different knowledge distillation algorithms.

End-to-end Knowledge Distillation Performance. As shown in Tables 1, 2, and 3, our teacher training method SoTeacher can improve the student’s test accuracy. Such improvements are significant and consistent across two datasets, teacher/student architecture pairs, and various knowledge distillation algorithms.

Ablation Study. As shown in Table 1 and 2, SoTeacher achieves the best performance on average when combining both consistent regularization (CR) and Lipschitz regularization (LR), as also demonstrated in our theoretical analyses.

Notably, our regularization methods, especially LR, will hurt the test accuracy of the teacher, despite the fact that it can improve the test accuracy of the student distilled from it. This echos our theoretical analyses that a Lipschitz constraint stronger than that bounds test set generalization is required for teacher to learn the true label distribution of the training set and converge towards student’s

Table 3: SoTeacher consistently outperforms Standard on CIFAR-100 with various KD algorithms.

	WRN40-2/WRN40-1		WRN40-2/WRN16-2		ResNet32x4/ShuffleV2	
	Standard	SoTeacher	Standard	SoTeacher	Standard	SoTeacher
FitNet	74.06 ± 0.20	74.88 ± 0.15	75.42 ± 0.38	75.64 ± 0.20	76.56 ± 0.15	77.91 ± 0.21
AT	73.78 ± 0.40	75.12 ± 0.17	75.45 ± 0.28	75.88 ± 0.09	76.20 ± 0.16	77.93 ± 0.15
SP	73.54 ± 0.20	74.71 ± 0.19	74.67 ± 0.37	75.94 ± 0.20	75.94 ± 0.16	78.06 ± 0.34
CC	73.46 ± 0.12	74.76 ± 0.16	75.08 ± 0.07	75.67 ± 0.39	75.43 ± 0.19	77.68 ± 0.28
VID	73.88 ± 0.30	74.89 ± 0.19	75.11 ± 0.07	75.71 ± 0.19	75.95 ± 0.11	77.57 ± 0.16
RKD	73.41 ± 0.47	74.66 ± 0.08	75.16 ± 0.21	75.59 ± 0.18	75.28 ± 0.11	77.46 ± 0.10
PKT	74.14 ± 0.43	74.89 ± 0.16	75.45 ± 0.09	75.53 ± 0.09	75.72 ± 0.18	77.84 ± 0.03
AB	73.93 ± 0.35	74.86 ± 0.10	70.09 ± 0.66	70.38 ± 0.87	76.27 ± 0.26	78.05 ± 0.21
FT	73.80 ± 0.15	74.75 ± 0.13	75.19 ± 0.15	75.68 ± 0.28	76.42 ± 0.17	77.56 ± 0.15
NST	73.95 ± 0.41	74.74 ± 0.14	74.95 ± 0.23	75.68 ± 0.16	76.07 ± 0.08	77.71 ± 0.10
CRD	74.44 ± 0.11	75.06 ± 0.37	75.52 ± 0.12	75.95 ± 0.02	76.28 ± 0.13	78.09 ± 0.13
SSKD	75.82 ± 0.22	75.94 ± 0.18	76.31 ± 0.07	76.32 ± 0.09	78.49 ± 0.10	79.37 ± 0.11
RCO	74.50 ± 0.32	74.81 ± 0.04	75.24 ± 0.34	75.50 ± 0.12	76.75 ± 0.13	77.59 ± 0.31

generalization. This also demonstrates that the success of our teacher training method is simply not due to better generalization of the teacher.

Other Knowledge Distillation Algorithms. Note that Table 3 includes various feature distillation algorithms such as FitNets, AT, SP, CC, VID, RKD, PKT, AB, FT, NST, CRD and SSKD. Although these distillation algorithms match all manner of features instead of predictions between teacher and student, they will achieve the best distillation performance when combined with the prediction distillation (*i.e.* original KD). Therefore, our teacher training method should still benefit the effectiveness of these distillation algorithms. We also experiment with a curriculum distillation algorithm RCO which distills from multiple checkpoints in teacher’s training trajectory. Our teacher training method should also benefit RCO as the later teacher checkpoints become more student-oriented. The results demonstrate that our SoTeacher can boost the distillation performance of almost all these distillation algorithms, which verifies its wide applicability.

Training overhead. Compared to standard teacher training, the computation overhead of SoTeacher is mainly due to the calculation of the Lipschitz constant, which is efficient as it only requires simple arithmetic calculation of the weights of trainable layers in a neural model (see Section 5). Empirically we observe that training with SoTeacher is slightly longer than the standard training for about 5%. The memory overhead of SoTeacher is incurred by buffering an average previous prediction for each input. However, since such prediction requires no gradient calculation we can store the buffer in a memory-mapped file.

7 Conclusion and Future Work

In this work we rigorously studied the feasibility to learn the true label distribution of the training data under a common empirical risk minimization framework. We also explore the favorable conditions that facilitate such learning. We believe our work is among the first attempts to establish a learning theory for an ideal teacher that is oriented towards the student performance in knowledge distillation. We believe our exploration can serve as a stepping stone to rethinking the teacher training and unleash the full potential of knowledge distillation.

In the future, we plan to adapt our theory and student-oriented teacher network training framework to other knowledge distillation scenarios such as transfer learning and mixture of experts.

References

Tiny imagenet, 2017. URL <https://www.kaggle.com/c/tiny-imagenet>.

Ahn, S., Hu, S. X., Damianou, A. C., Lawrence, N. D., and Dai, Z. Variational information distillation for knowledge transfer. *CVPR*, pp. 9155–9163, 2019.

Bartlett, P. L., Foster, D. J., and Telgarsky, M. Spectrally-normalized margin bounds for neural networks. In *NIPS*, 2017.

- Berthelot, D., Carlini, N., Cubuk, E. D., Kurakin, A., Sohn, K., Zhang, H., and Raffel, C. Remix-match: Semi-supervised learning with distribution alignment and augmentation anchoring. *ArXiv*, abs/1911.09785, 2019.
- Brier, G. W. Verification of forecasts expressed in terms of probability. *Monthly Weather Review*, 78: 1–3, 1950.
- Buciluă, C., Caruana, R., and Niculescu-Mizil, A. Model compression. In *Proceedings of the 12th ACM SIGKDD international conference on Knowledge discovery and data mining*, pp. 535–541, 2006.
- Cho, J. H. and Hariharan, B. On the efficacy of knowledge distillation. *ICCV*, pp. 4793–4801, 2019.
- Dao, T., Kamath, G. M., Syrgkanis, V., and Mackey, L. W. Knowledge distillation as semiparametric inference. *ArXiv*, abs/2104.09732, 2021.
- Deng, J., Dong, W., Socher, R., Li, L.-J., Li, K., and Fei-Fei, L. Imagenet: A large-scale hierarchical image database. In *CVPR*, 2009.
- Dong, C., Liu, L., and Shang, J. Double descent in adversarial training: An implicit label noise perspective. *ArXiv*, abs/2110.03135, 2021.
- Furlanello, T., Lipton, Z. C., Tschannen, M., Itti, L., and Anandkumar, A. Born again neural networks. In *ICML*, 2018.
- Geifman, Y., Uziel, G., and El-Yaniv, R. Bias-reduced uncertainty estimation for deep neural classifiers. In *ICLR*, 2019.
- Gneiting, T. and Raftery, A. E. Strictly proper scoring rules, prediction, and estimation. *Journal of the American Statistical Association*, 102:359 – 378, 2007.
- Gouk, H., Frank, E., Pfahringer, B., and Cree, M. J. Regularisation of neural networks by enforcing lipschitz continuity. *Machine Learning*, 110:393–416, 2021.
- Guo, C., Pleiss, G., Sun, Y., and Weinberger, K. Q. On calibration of modern neural networks. *ArXiv*, abs/1706.04599, 2017.
- Hao, Z., Lu, C., Hu, Z., Wang, H., Huang, Z., Liu, Q., Chen, E., and Lee, C. Asgn: An active semi-supervised graph neural network for molecular property prediction. *Proceedings of the 26th ACM SIGKDD International Conference on Knowledge Discovery & Data Mining*, 2020.
- He, K., Zhang, X., Ren, S., and Sun, J. Deep residual learning for image recognition. *CVPR*, pp. 770–778, 2016.
- Hendrycks, D., Mu, N., Cubuk, E. D., Zoph, B., Gilmer, J., and Lakshminarayanan, B. Augmix: A simple data processing method to improve robustness and uncertainty. *ArXiv*, abs/1912.02781, 2020.
- Heo, B., Lee, M., Yun, S., and Choi, J. Y. Knowledge transfer via distillation of activation boundaries formed by hidden neurons. In *AAAI*, 2019.
- Hinton, G. E., Vinyals, O., and Dean, J. Distilling the knowledge in a neural network. *ArXiv*, abs/1503.02531, 2015.
- Huang, Z. and Wang, N. Like what you like: Knowledge distill via neuron selectivity transfer. *ArXiv*, abs/1707.01219, 2017.
- Jin, X., Peng, B., Wu, Y., Liu, Y., Liu, J., Liang, D., Yan, J., and Hu, X. Knowledge distillation via route constrained optimization. *ICCV*, pp. 1345–1354, 2019.
- Kim, J., Park, S., and Kwak, N. Paraphrasing complex network: Network compression via factor transfer. *ArXiv*, abs/1802.04977, 2018.
- Krizhevsky, A. Learning multiple layers of features from tiny images. 2009.

- Laine, S. and Aila, T. Temporal ensembling for semi-supervised learning. *ArXiv*, abs/1610.02242, 2017.
- Lakshminarayanan, B., Pritzel, A., and Blundell, C. Simple and scalable predictive uncertainty estimation using deep ensembles. In *NIPS*, 2017.
- Liu, J., Shou, L., Pei, J., Gong, M., Yang, M., and Jiang, D. Cross-lingual machine reading comprehension with language branch knowledge distillation. In *COLING*, 2020.
- Matsubara, Y. torchdistill: A modular, configuration-driven framework for knowledge distillation. In *International Workshop on Reproducible Research in Pattern Recognition*, pp. 24–44. Springer, 2021.
- Menon, A. K., Rawat, A. S., Reddi, S. J., Kim, S., and Kumar, S. A statistical perspective on distillation. In *ICML*, 2021.
- Miyato, T., Kataoka, T., Koyama, M., and Yoshida, Y. Spectral normalization for generative adversarial networks. *ArXiv*, abs/1802.05957, 2018.
- Moon, J., Kim, J., Shin, Y., and Hwang, S. Confidence-aware learning for deep neural networks. In *ICML*, 2020.
- Müller, R., Kornblith, S., and Hinton, G. E. When does label smoothing help? In *NeurIPS*, 2019.
- Naeini, M. P., Cooper, G. F., and Hauskrecht, M. Obtaining well calibrated probabilities using bayesian binning. *Proceedings of the ... AAAI Conference on Artificial Intelligence. AAAI Conference on Artificial Intelligence*, 2015:2901–2907, 2015.
- Neal, R. M. Pattern recognition and machine learning. *Technometrics*, 49:366 – 366, 2007.
- Park, D. Y., Cha, M., Jeong, C., Kim, D., and Han, B. Learning student-friendly teacher networks for knowledge distillation. *ArXiv*, abs/2102.07650, 2021.
- Park, W., Kim, D., Lu, Y., and Cho, M. Relational knowledge distillation. *CVPR*, pp. 3962–3971, 2019.
- Passalis, N. and Tefas, A. Learning deep representations with probabilistic knowledge transfer. In *ECCV*, 2018.
- Peng, B., Jin, X., Liu, J., Zhou, S., Wu, Y., Liu, Y., Li, D., and Zhang, Z. Correlation congruence for knowledge distillation. *ICCV*, pp. 5006–5015, 2019.
- Qian, J., Fruit, R., Pirotta, M., and Lazaric, A. Concentration inequalities for multinoulli random variables. *ArXiv*, abs/2001.11595, 2020.
- Romero, A., Ballas, N., Kahou, S. E., Chassang, A., Gatta, C., and Bengio, Y. Fitnets: Hints for thin deep nets. *CoRR*, abs/1412.6550, 2015.
- Shah, H., Khare, A., Shah, N., and Siddiqui, K. Kd-lib: A pytorch library for knowledge distillation, pruning and quantization, 2020.
- Sohn, K., Berthelot, D., Li, C.-L., Zhang, Z., Carlini, N., Cubuk, E. D., Kurakin, A., Zhang, H., and Raffel, C. Fixmatch: Simplifying semi-supervised learning with consistency and confidence. *ArXiv*, abs/2001.07685, 2020.
- Sokolich, J., Giryas, R., Sapiro, G., and Rodrigues, M. R. D. Robust large margin deep neural networks. *IEEE Transactions on Signal Processing*, 65:4265–4280, 2017.
- Szegedy, C., Vanhoucke, V., Ioffe, S., Shlens, J., and Wojna, Z. Rethinking the inception architecture for computer vision. *CVPR*, pp. 2818–2826, 2016.
- Tan, M., Chen, B., Pang, R., Vasudevan, V., and Le, Q. V. Mnasnet: Platform-aware neural architecture search for mobile. *CVPR*, pp. 2815–2823, 2019.

- Tang, J. and Wang, K. Ranking distillation: Learning compact ranking models with high performance for recommender system. *Proceedings of the 24th ACM SIGKDD International Conference on Knowledge Discovery & Data Mining*, 2018.
- Thulasidasan, S., Chennupati, G., Bilmes, J. A., Bhattacharya, T., and Michalak, S. E. On mixup training: Improved calibration and predictive uncertainty for deep neural networks. In *NeurIPS*, 2019.
- Tian, Y., Krishnan, D., and Isola, P. Contrastive representation distillation. *ArXiv*, abs/1910.10699, 2020.
- Tung, F. and Mori, G. Similarity-preserving knowledge distillation. *ICCV*, pp. 1365–1374, 2019.
- Wang, Q., Yang, L., Kanagal, B., Sanghai, S. K., Sivakumar, D., Shu, B., Yu, Z., and Elsas, J. L. Learning to extract attribute value from product via question answering: A multi-task approach. *Proceedings of the 26th ACM SIGKDD International Conference on Knowledge Discovery & Data Mining*, 2020.
- Weissman, T., Ordentlich, E., Seroussi, G., Verdú, S., and Weinberger, M. J. Inequalities for the 11 deviation of the empirical distribution. 2003.
- Xie, Q., Dai, Z., Hovy, E. H., Luong, M.-T., and Le, Q. V. Unsupervised data augmentation for consistency training. *arXiv: Learning*, 2020.
- Xu, G., Liu, Z., Li, X., and Loy, C. C. Knowledge distillation meets self-supervision. In *ECCV*, 2020.
- Yang, C., Xie, L., Qiao, S., and Yuille, A. L. Training deep neural networks in generations: A more tolerant teacher educates better students. In *AAAI*, 2019.
- Yang, Z., Shou, L., Gong, M., Lin, W., and Jiang, D. Model compression with two-stage multi-teacher knowledge distillation for web question answering system. *Proceedings of the 13th International Conference on Web Search and Data Mining*, 2020.
- Yoshida, Y. and Miyato, T. Spectral norm regularization for improving the generalizability of deep learning. *ArXiv*, abs/1705.10941, 2017.
- Zagoruyko, S. and Komodakis, N. Wide residual networks. *ArXiv*, abs/1605.07146, 2016.
- Zagoruyko, S. and Komodakis, N. Paying more attention to attention: Improving the performance of convolutional neural networks via attention transfer. *ArXiv*, abs/1612.03928, 2017.
- Zhang, H., Cissé, M., Dauphin, Y., and Lopez-Paz, D. mixup: Beyond empirical risk minimization. *ArXiv*, abs/1710.09412, 2018a.
- Zhang, X., Zhou, X., Lin, M., and Sun, J. Shufflenet: An extremely efficient convolutional neural network for mobile devices. *CVPR*, pp. 6848–6856, 2018b.
- Zhang, Y., Xu, X., Zhou, H., and Zhang, Y. Distilling structured knowledge into embeddings for explainable and accurate recommendation. *Proceedings of the 13th International Conference on Web Search and Data Mining*, 2020.

A Proof of Theorem 4.1

Step I: Bound the difference between the true label distribution and the sample mean. First we note that the set of all training inputs can be grouped into several subsets such that the inputs in each subset possess similar true label distribution.

More formally, Let $\mathcal{C}^r = \{\bar{x}_j\}_{j=1}^{N_r}$ be an r -external covering of \mathcal{S} with minimum cardinality, namely

$$\mathcal{S} \subseteq \bigcup_{x \in \mathcal{C}^r} \{x' \mid \|x' - x\| \leq r\}, \quad (15)$$

where we refer \bar{x}_j as the covering center, and N_r is the covering number.

Let $\{\mathcal{S}_j^r\}_{j=1}^{N_r}$ be any disjoint partition of \mathcal{S} such that $\mathcal{S}_j^r \subseteq \{x' \mid \|x' - \bar{x}_j\| \leq r\}$. We show that \mathcal{S}_j^r attains a property that the true label distribution $\mathbf{p}^*(x)$ of any input x in this subset will not be too far from the sample mean of one-hot labels $\bar{\mathbf{y}}_j = |\mathcal{S}_j^r|^{-1} \sum_{x \in \mathcal{S}_j^r} \mathbf{1}_y$ in this subset. Namely given any $\varepsilon > 0$, we have

$$P(\|\mathbf{p}^*(x) - \bar{\mathbf{y}}_j\| \geq \varepsilon) \leq 2 \exp\left(-\frac{|\mathcal{S}_j^r|}{2K} \tilde{\varepsilon}^2\right), \quad (16)$$

where $\tilde{\varepsilon} = \max(\varepsilon - 2L^*r, 0)$.

To prove this property we first present two lemmas.

Lemma A.1 (Lipschitz constraint of the true label distribution). *Let \mathcal{S}_j^r be a subset constructed above and $\bar{\mathbf{y}}_j = |\mathcal{S}_j^r|^{-1} \sum_{x \in \mathcal{S}_j^r} \mathbf{1}_y$. Then for any $x \in \mathcal{S}_j^r$ we have,*

$$\|\mathbf{p}^*(x) - \mathbb{E}[\bar{\mathbf{y}}_j]\| \leq 2L^*r. \quad (17)$$

Proof. First, since $x \in \mathcal{S}_j^r$, we have $\|x - \bar{x}_j\| \leq r$, which implies $\|\mathbf{p}^*(x) - \mathbf{p}^*(\bar{x}_j)\| \leq L^*r$ by the locally Lipschitz continuity of \mathbf{p}^* . Then for any $x, x' \in \mathcal{S}_j^r$, we will have $\|\mathbf{p}^*(x) - \mathbf{p}^*(x')\| \leq 2L^*r$ by the triangle inequality. Let $N_S = |\mathcal{S}_j^r|$. Therefore,

$$\left\| \mathbf{p}^*(x) - \frac{1}{N_S} \sum_{x \in \mathcal{S}_j^r} \mathbf{p}^*(x) \right\| \leq 2 \frac{N_S - 1}{N_S} L^*r \leq 2L^*r. \quad (18)$$

Further, the linearity of the expectation implies

$$\mathbb{E}[\bar{\mathbf{y}}] = N_S^{-1} \sum_{x \in \mathcal{S}_j^r} \mathbb{E}[\mathbf{1}_{y(x)}] = N_S^{-1} \sum_{x \in \mathcal{S}_j^r} \mathbf{p}^*(x). \quad (19)$$

Therefore $\|\mathbf{p}^*(x) - \mathbb{E}[\bar{\mathbf{y}}_j]\| \leq 2L^*r$. \square

Lemma A.2 (Concentration inequality of the sample mean). *Let \mathcal{S} be a set of x with cardinality N . Let $\bar{\mathbf{y}} = N^{-1} \sum_{x \in \mathcal{S}} \mathbf{1}_y$ be the sample mean. Then for any p -norm $\|\cdot\|$ and any $\varepsilon > 0$, we have*

$$P(\|\bar{\mathbf{y}} - \mathbb{E}[\bar{\mathbf{y}}]\| \geq \varepsilon) \leq 2 \exp\left(-\frac{N}{2K} \varepsilon^2\right). \quad (20)$$

Proof. Note that $\bar{\mathbf{y}}$ obeys a multinomial distribution, i.e. $\bar{\mathbf{y}} \sim N^{-1} \text{multinomial}(N, \mathbb{E}[\bar{\mathbf{y}}])$. We utilize the classic results on the concentration properties of multinomial distribution based on ℓ_1 norm Weissman et al. (2003); Qian et al. (2020), namely

$$P(\|\bar{\mathbf{y}} - \mathbb{E}[\bar{\mathbf{y}}]\|_1 \geq \varepsilon) \leq 2 \exp\left(-\frac{N}{2K} \varepsilon^2\right) \quad (21)$$

Further, for any $\mathbf{q} \in \mathbb{R}^K$, by the equivalence of p -norm we have $\|\mathbf{q}\| \leq \|\mathbf{q}\|_1$. Therefore,

$$\{\mathbf{q} \mid \|\mathbf{q}\| \geq \varepsilon\} \subseteq \{\mathbf{q} \mid \|\mathbf{q}\|_1 \geq \varepsilon\}, \quad (22)$$

which implies,

$$P(\|\mathbf{q}\| \geq \varepsilon) \leq P(\|\mathbf{q}\|_1 \geq \varepsilon). \quad (23)$$

Combine inequality (21) and (23) we then have (20). \square

One can see that Lemma A.1 bounds the difference between true label distribution of individual inputs and the mean true label distribution, while Lemma A.2 bounds the difference between the sample mean and the mean true label distribution. Therefore the difference between the true label distribution and the sample mean is also bounded, since by the triangle inequality we have

$$\|\mathbf{p}^*(x) - \bar{\mathbf{y}}\| \leq \|\mathbf{p}^*(x) - \mathbb{E}[\bar{\mathbf{y}}]\| + \|\bar{\mathbf{y}} - \mathbb{E}[\bar{\mathbf{y}}]\|. \quad (24)$$

This implies

$$P(\|\mathbf{p}^*(x) - \bar{\mathbf{y}}\| \geq \varepsilon) \leq P(\|\bar{\mathbf{y}} - \mathbb{E}[\bar{\mathbf{y}}]\| \geq \tilde{\varepsilon}), \quad (25)$$

where $\tilde{\varepsilon} = \max(\varepsilon - 2L^*r, 0)$. Apply Lemma A.2 we then have (16).

Step II: Bound the difference between the prediction given by the empirical risk minimizer and the sample mean.

Here we show that given the locally Lipschitz constraint established in each disjoint partition we constructed above, the prediction given by the empirical risk minimizer will be close to the sample mean. As an example, we focus on the negative log-likelihood loss, namely $\ell(\mathbf{f}(x), y) = -\mathbf{1}_y \cdot \log \mathbf{f}(x)$. Other loss functions that are subject to the proper scoring rule can be investigated in a similar manner.

First, we regroup the sum in (5) based on the partition constructed above, namely

$$\hat{R}(\mathbf{f}, \mathcal{S}) = \frac{1}{N_r} \sum_{j=1}^{N_r} \hat{R}(\mathbf{f}, \mathcal{S}_j^r), \quad (26)$$

where $\hat{R}(\mathbf{f}, \mathcal{S}_j^r) = -|\mathcal{S}_j^r|^{-1} \sum_{i=1}^{|\mathcal{S}_j^r|} \mathbf{1}_{y_i} \cdot \log \mathbf{f}(x_i)$ is the empirical risk in each partition. Since we are only concerned with the existence of a desired minimizer of the empirical risk, we can view \mathbf{f} as able to achieve any labeling of the training inputs that suffices the local Lipschitz constraint. Thus the empirical risk minimization is equivalent to the minimization of the empirical risk in each partition. The problem can thus be defined as, for each $j = 1, \dots, N_r$,

$$\begin{aligned} \min_{\mathbf{f}} \quad & \hat{R}(\mathbf{f}, \mathcal{S}_j^r) \\ \text{s.t.} \quad & \|\mathbf{f}(x) - \mathbf{f}(\bar{x}_j)\| \leq Lr, \forall x \in \mathcal{S}_j^r, \end{aligned} \quad (27)$$

where the constraint is imposed by the locally-Lipschitz continuity of \mathbf{f} . By the following lemma, we show that the minimizer of such problem is achieved only if $\mathbf{f}(\bar{x}_j)$ is close to the sample mean.

Lemma A.3. *Let $\bar{\mathbf{y}} = |\mathcal{S}_j^r|^{-1} \sum_{x \in \mathcal{S}_j^r} \mathbf{1}_y$. The minimum of the problem (27) is achieved only if $\mathbf{f}(\bar{x}_j) = \bar{\mathbf{y}}_j(1 + K Lr) - Lr$.*

Proof. We note that since the loss function we choose is strongly convex, to minimize the empirical risk, the prediction of any input x must be as close to the one-hot labeling as possible. Therefore the problem (27) can be formulated into a vector minimization where we can employ Karush–Kuhn–Tucker (KKT) theorem to find the necessary conditions of the minimizer.

We rephrase the problem (27) as

$$\begin{aligned} \min_{\{\mathbf{p}_i\}_{i=1}^N} \quad & -\frac{1}{N} \sum_i \mathbf{1}_{y_i} \cdot \log \mathbf{p}_i \\ \text{s.t.} \quad & \|\mathbf{p}_i - \mathbf{p}\| \leq \varepsilon, \sum_k \mathbf{p}_i^k = 1, \sum_k \mathbf{p}^k = 1, \mathbf{p}_i^k \geq 0, \mathbf{p}^k \geq 0. \end{aligned} \quad (28)$$

Case I. We first discuss the case when $\mathbf{p}^k + \varepsilon < 1$ for all k . First, we observe that for any \mathbf{p} , the minimum of the above problem is achieved only if $\mathbf{p}_i^{y_i} = \mathbf{p}^{y_i} + \varepsilon$. Because by contradiction, if $\mathbf{p}_i^{y_i} < \mathbf{p}^{y_i} + \varepsilon$, we will have $-\log \mathbf{p}_i^{y_i} > -\log(\mathbf{p}^{y_i} + \varepsilon)$, and $\mathbf{p}^{y_i} + \varepsilon$ belongs to the feasible set, which means $\mathbf{p}_i^{y_i}$ does not attain the minimum.

The above problem can then be rephrased as

$$\min_{\mathbf{p}} -\frac{1}{N} \sum_i \log(\mathbf{p}^{y_i} + \varepsilon), \text{ s.t. } \sum_k \mathbf{p}^k = 1, \mathbf{p}^k \geq 0, \quad (29)$$

where we have neglected the condition associated with $\mathbf{p}_i^{k \neq y_i}$, since they do not contribute to the objective, they can be chosen arbitrarily as long as the constraints are sufficed, and clearly the constraints are underdetermined.

Let $N_k = \sum_i 1(y_i = k)$, we have $\sum_i \log(\mathbf{p}^{y_i} + \varepsilon) = \sum_k N_k \log(\mathbf{p}^k + \varepsilon)$. Therefore the above problem is equivalent to

$$\min_{\mathbf{p}} - \sum_k \bar{y}^k \log(\mathbf{p}^k + \varepsilon), \quad s.t. \quad \sum_k \mathbf{p}^k = 1, \mathbf{p}^k \geq 0, \quad (30)$$

where $\bar{\mathbf{y}} \equiv [N_1/N, \dots, N_k/N]^T$ is equal to the sample mean $N^{-1} \sum_i \mathbf{1}_{y_i}$.

To solve the strongly convex minimization problem (30) it is easy to employ KKT conditions to show that

$$\mathbf{p} = \bar{\mathbf{y}}(1 + K\varepsilon) - \varepsilon.$$

Case II. We now discuss the case when $\hat{\mathbf{p}}$ is the minimizer of (28) and there exists k' such that $\hat{\mathbf{p}}^{k'} + \varepsilon \geq 1$. And $\hat{\mathbf{p}} \neq \mathbf{p}^*$, where $\mathbf{p}^* = \bar{\mathbf{y}}(1 + K\varepsilon) - \varepsilon$ is the form of the minimizer in the previous case.

Considering a non-trivial case $\mathbf{p}^{*k'} < 1 - \varepsilon$. Otherwise the true label distribution is already close to the one-hot labeling, which is the minimizer of the empirical risk. Therefore by $\sum_{k \neq k'} \mathbf{p}^{*k} > \varepsilon$ we have the condition

$$\sum_{k \neq k'} \bar{y}^k > \frac{K\varepsilon}{1 + K\varepsilon} \quad (31)$$

Now considering the minimization objective $R(p) = -N^{-1} \sum_i \mathbf{1}_{y_i} \cdot \log \mathbf{p}_i$. For all i with $y_i = k'$, we must have $\mathbf{p}_i^{y_i} = 1$, otherwise the optimal cannot be attained by contradiction. Then the minimization problem can be rephrased as

$$\min \sum_{k \neq k'} \bar{y}^k \log(\hat{\mathbf{p}}^k + \varepsilon), \quad s.t. \quad \sum_{k' \neq k} \hat{\mathbf{p}}^k \geq \varepsilon, \hat{\mathbf{p}}^k \geq 0, \quad (32)$$

where the first constraint is imposed by $\hat{\mathbf{p}}^{k'} \geq 1 - \varepsilon$.

Employ KKT conditions similarly we can have $\hat{\mathbf{p}}^k = \bar{y}^k / \lambda - \varepsilon$ where λ is a constant. By checking the constraint we can derive $\lambda \geq \sum_k \bar{y}^k / (K\varepsilon)$.

However, the minimization objective

$$\min_{\lambda} - \sum_{k \neq k'} \bar{y}^k \log \frac{\bar{y}^k}{\lambda},$$

requires λ to be minimized. Therefore $\lambda = \sum_{k \neq k'} \bar{y}^k / (K\varepsilon)$, which implies

$$\hat{\mathbf{p}}^k = K\varepsilon \frac{\bar{y}^k}{\sum_{k \neq k'} \bar{y}^k} - \varepsilon. \quad (33)$$

Now since $\hat{\mathbf{p}} = \arg \min_p R(p)$ and $\hat{\mathbf{p}} \neq \mathbf{p}^*$, we must have $R(\hat{\mathbf{p}}) < R(\mathbf{p}^*)$. This means

$$- \sum_{k \neq k'} \bar{y}^k \log \frac{K\varepsilon \bar{y}^k}{\sum_{k \neq k'} \bar{y}^k} < - \sum_{k \neq k'} \bar{y}^k \log[\bar{y}^k(1 + K\varepsilon)], \quad (34)$$

which is reduced to

$$\sum_{k \neq k'} \bar{y}^k < \frac{K\varepsilon}{1 + K\varepsilon} \quad (35)$$

But this is contradict to our assumption. \square

We are now be able to bound the difference between the predictions of the training inputs produced by the empirical risk minimizer and the sample mean in each \mathcal{S}_j^r . To see that we have for each $x \in \mathcal{S}_j^r$.

$$\begin{aligned} \|\mathbf{f}(x) - \bar{\mathbf{y}}_j\| &\leq \|\mathbf{f}(x) - \mathbf{f}(\bar{x}_j)\| + \|\mathbf{f}(\bar{x}_j) - \bar{\mathbf{y}}_j\| \\ &\leq Lr(1 + K\|\bar{\mathbf{y}}_j - K^{-1}\mathbf{1}\|) \\ &\leq Lr(1 + K\|\mathbf{1}_{(\cdot)} - K^{-1}\mathbf{1}\|). \end{aligned} \quad (36)$$

By Equation (16) we then have for any $x \in \mathcal{S}_j^r$,

$$P(\|\mathbf{f}(x) - \mathbf{p}^*(x)\| \geq \varepsilon) \leq 2 \exp\left(-\frac{|\mathcal{S}_j^r|}{2K} \tilde{\varepsilon}^2\right), \quad (37)$$

which means the difference between the predictions and the true label distribution is also bounded. Here $\tilde{\varepsilon} = \max(\varepsilon - Lr(1 + K\|\mathbf{1}_{(\cdot)} - K^{-1}\mathbf{1}\|) - 2L^*r, 0)$.

Step III: Show the disjoint partition is non-trivial. In (37), we have managed to bound the difference between the predictions yielded by an empirical risk minimizer and the true label distribution based on the cardinality of the subset $|\mathcal{S}_j^r|$, namely the number of inputs in j -partition. However $|\mathcal{S}_j^r|$ is critical to the bound here as if $|\mathcal{S}_j^r| = 1$, then (37) becomes a trivial bound. Here we show $|\mathcal{S}_j^r|$ is non-negligible based on simple combinatorics.

Lemma A.4. *Let $\{\mathcal{S}_j^r\}_{j=1}^{N^r}$ be a disjoint partition of the entire training set \mathcal{S} . Denote $\mathcal{S}^r(x)$ as the partition that includes x . Let $N(x) = |\mathcal{S}^r(x)|$ and $N = |\mathcal{S}|$. Then for any $\kappa \geq 1$,*

$$\left| \left\{ x \mid N(x) \geq \frac{N}{\kappa N^r} \right\} \right| \geq \left(1 - \frac{1}{\kappa} + \frac{1}{\kappa N^r} \right) N. \quad (38)$$

Proof. We note that the problem is to show the minimum number of x such that $N(x) \geq N/(\kappa N^r)$. This is equivalent to find the maximum number of x such that $N(x) \leq N/(\kappa N^r)$. Since we only have N^r subsets, the maximum can be attained only if for $N^r - 1$ subsets \mathcal{S}^r , $|\mathcal{S}^r| = N/(\kappa N^r)$. Otherwise, if for any one of these subsets $|\mathcal{S}^r| < N/(\kappa N^r)$, then it is always feasible to let $|\mathcal{S}^r| = N/(\kappa N^r)$ and the maximum increases. Similarly, if the number of such subsets is less than $N^r - 1$, then it is always feasible to let another subset subject to $|\mathcal{S}^r| = N/(\kappa N^r)$ and the maximum increases. We can then conclude that at most $N(N^r - 1)/(\kappa N^r)$ inputs can have the property $N(x) \leq N/(\kappa N^r)$. \square

The above lemma basically implies when partitioning N inputs into N^r subsets, a large fraction of the inputs will be assigned to a subset with cardinality at least $N/(\kappa N^r)$. Here N^r is the covering number and is bounded above based on the property of the covering in the Euclidean space. Apply Lemma A.4 to (37) we then arrive at Theorem 4.1.

Difference from the Lipschitz bound in generalization theory. We note that in Theorem 4.1, the constraint on the local Lipschitz continuity of the hypothesis function is more strict than that is required in typical generalization theory of deep neural networks Sokolic et al. (2017); Bartlett et al. (2017).

Remark A.5. *In generalization theory we often require the hypothesis function to be locally Lipschitz continuous around training inputs, such that the difference between the prediction of an unseen input and the prediction of its nearest training input is bounded. However, for learning true label distribution of the training data we need to bound the difference between the predictions of a subset of training inputs. Therefore, our constraint requires the Lipschitz continuity to be established at a larger scale in the input space.*

Indeed, we observe from later experiments that our stronger Lipschitz constraint will actually hurt the performance of the teacher on the test set, whereas it can still improve the student performance.

B Limitations

In this paper we focus on the theoretical feasibility of learning the true label distribution of training examples with empirical risk minimization. Therefore we only analyze the existence of such a desired minimizer, but neglect the optimization process to achieve it. By explore the optimization towards true label distribution, potentially more dynamics can be found to inspire new regularization techniques.

Also, our proposed method for training a student-oriented teacher may not be able to advance the state-of-the-art significantly, as the regularization techniques based inspired by our analyses such as Lipschitz regularization and consistency regularization may more or less leveraged by existing training practice of deep neural networks, either implicitly or explicitly.

Table 4: β for different feature distillation algorithms

	β			β			β	
	Standard	SoTeacher		Standard	SoTeacher		Standard	SoTeacher
FitNets	100	50	AT	1000	500	SP	3000	1500
CC	0.02	0.01	VID	1.0	0.5	RKD	1.0	0.5
PKT	30000	15000	AB	1.0	0.5	FT	200	100
NST	50	25	CRD	0.8	0.5			

C Details of experiment setting

C.1 Hyperparameter setting for teacher network training

For all the experiments on CIFAR-100, we employ SGD as the optimizer and train for 240 epochs with a batch size of 64. The learning rate is initialized at 0.05 and decayed by a factor of 10 at the epochs 150, 180 and 210, with an exception for ShuffleNet where the learning rate is initialized at 0.01 following existing practice Tian et al. (2020); Park et al. (2021). The weight decay and momentum are fixed as 0.0005 and 0.9 respectively. The training images are augmented with random cropping and random horizontal flipping with a probability of 0.5.

For Tiny-ImageNet experiments, we employ SGD as the optimizer and conduct the teacher training for 90 epochs with a batch size of 128. The learning rate starts at 0.1 and is decayed by a factor of 10 at epochs 30 and 60. The weight decay and momentum are fixed as 0.0005 and 0.9 respectively. The training images are augmented with random rotation with a maximum degree of 20, random cropping and random horizontal flipping with a probability of 0.5. For student training the only difference is that we train for additional 10 epochs, with one more learning rate decay at epoch 90, aligned with previous settings Tian et al. (2020).

C.2 Hyperparameter setting for knowledge distillation algorithms

For knowledge distillation algorithms we refer to the setting in RepDistiller¹. Specifically, for original KD, the loss function used for student training is defined as

$$\ell = \alpha \ell_{\text{Cross-Entropy}} + (1 - \alpha) \ell_{KD}.$$

We grid search the best hyper-parameters that achieve the optimal performance, namely the loss scaling ratio α is set as 0.5 and the temperature is set as 4 for both CIFAR-100 and Tiny-ImageNet. For all feature distillation methods combined with KD the loss function can be summarized as Tian et al. (2020)

$$\ell = \gamma \ell_{\text{Cross-Entropy}} + \alpha \ell_{KD} + \beta \ell_{\text{Distill}},$$

where we grid search the optimal γ and α to be 1.0 and 1.0 respectively. When using our teacher training method, all these hyperparameters are kept same except that for all feature distillation algorithms the scaling weights corresponding to the feature distillation losses β are cut by half, as we wish to rely more on the original KD that is well supported by our theoretical understanding. Table 4 list β used in our experiments for all feature distillation algorithms. For SSKD Xu et al. (2020) the hyperparameters are set as $\lambda_1 = 1.0$, $\lambda_2 = 1.0$, $\lambda_3 = 2.7$, $\lambda_4 = 10.0$ for standard training and $\lambda_1 = 1.0$, $\lambda_2 = 1.0$, $\lambda_3 = 1.0$, $\lambda_4 = 10.0$ for our methods. For the curriculum distillation algorithm RCO we experiment based on one-stage EEI (equal epoch interval). We select 24 anchor points (or equivalently every 10 epochs) from the teacher’s saved checkpoints.

D Experiments with uncertainty regularization methods on unseen data

Experiment setup. We conduct experiments on CIFAR-100 with teacher-student pair WRN40-2/WRN40-1. We employ the original KD as the distillation algorithm. The hyperparameter settings are the same as those mentioned in the main results (see Appendix C). For each regularization method we grid search the hyperparameter that yields the best student performance. The results are summarized in Table 5.

¹<https://github.com/HobbitLong/RepDistiller>

Table 5: Performance of the knowledge distillation when training the teacher using existing regularization methods for learning quality uncertainty on unseen data.

	WRN40-2/WRN40-1	
	Student	Teacher
Standard	73.73 ± 0.13	76.38 ± 0.13
SoTeacher	74.35 ± 0.23	74.95 ± 0.28
ℓ_2 (5×10^{-4})	73.73 ± 0.13	76.38 ± 0.13
ℓ_1 (10^{-5})	73.60 ± 0.15	73.52 ± 0.05
Mixup ($\alpha = 0.2$)	73.19 ± 0.21	77.30 ± 0.20
Cutmix ($\alpha = 0.2$)	73.61 ± 0.26	78.42 ± 0.07
Augmix ($\alpha = 1, k = 3$)	73.83 ± 0.09	77.80 ± 0.30
CRL ($\lambda = 1$)	74.13 ± 0.29	76.69 ± 0.16

Classic regularization. We observe that with stronger ℓ_2 or ℓ_1 regularization the student performance will not deteriorate significantly as teacher converges. However, it also greatly reduces the performance of the teacher. Subsequently the performance of the student is not improved as shown in Table 5.

Label smoothing. Label smoothing is shown to not only improve the performance but also the uncertainty estimates of deep neural networks Müller et al. (2019). However, existing works have already shown that label smoothing can hurt the effectiveness of knowledge distillation Müller et al. (2019), thus we neglect the results here. An intuitive explanation is that label smoothing encourages the representations of samples to lie in equally separated clusters, thus “erasing” the information encoding possible secondary classes in a sample Müller et al. (2019).

Data augmentation. Previous works have demonstrated that mixup-like data augmentation techniques can greatly improve the uncertainty estimation on unseen data Thulasidasan et al. (2019); Hendrycks et al. (2020). For example, Mixup augmented the training samples as $x := \alpha x + (1 - \alpha)x'$, and $y := \alpha y + (1 - \alpha)y'$, where (x', y') is a randomly drawn pair not necessarily belonging to the same class as x .

As shown in Table 5, stronger mixup can improve the performance of the teacher, whereas it can barely improve or even hurt the performance of the student. Based on our theoretical understanding (Theorem 4.2), we conjecture the reason might be that mixup distorts the true label distribution of an input stochastically throughout the training, thus hampering the learning of true label distribution.

Temperature scaling. Previous works have suggested using the uncertainty on a validation set to tune the temperature for knowledge distillation either in standard learning Menon et al. (2021) or robust learning Dong et al. (2021). However, the optimal temperature may not be well aligned with that selected based on uncertainty Menon et al. (2021). We neglect the experiment results here as the distillation temperature in our experiments is already fine-tuned.

Uncertainty learning. CRL designs the loss function as $\ell = \ell_{\text{CE}} + \lambda \ell_{\text{CRL}}$, where ℓ_{CE} is the cross-entropy loss and ℓ_{CRL} is an additional regularization term bearing the form of

$$\ell_{\text{CRL}} = \max(0, -g(c(x_i), c(x_j))(p(x_i) - p(x_j)) + |c(x_i) - c(x_j)|), \quad (39)$$

where $p(x) = \max_k \mathbf{f}(x)^k$ is the maximum probability of model’s prediction on a training sample x and

$$c(x) = \frac{1}{t-1} \sum_{t'=1}^{t-1} 1(\arg \max_k \mathbf{f}(x)_{t'}^k = y)$$

is the frequency of correct predictions through the training up to the current epoch. Here $g(c_i, c_j) = 1$ if $c_i > c_j$ and $g(c_i, c_j) = -1$ otherwise. Although originally proposed to improve the uncertainty quality of deep neural networks in terms of ranking, we found that CRL with a proper hyperparameter can improve the distillation performance, as shown in Table 5.

We note that the effectiveness of CRL on distillation can be interpreted by our theoretical understanding, as its regularization term (39) is essentially a special form of consistency regularization. To see this we first notice (39) is a margin loss penalizing the difference between $p(x)$ and $c(x)$ in terms of

ranking. We then rewrite $c(x)$ as

$$c(x) = \mathbf{1}_y \cdot \frac{1}{t-1} \sum_{t'=1}^{t-1} \text{Onehot}[\mathbf{f}(x)_{t'}], \quad (40)$$

which is similar to our consistency regularization target (12) except the prediction is first converted into one-hot encoding. Such variation may not be the best for knowledge distillation as we wish those secondary class probabilities in the prediction be aligned as well.